Optics Letters

Experimental demonstration of structural robustness of spatially partially coherent fields in turbulence

Abhinandan Bhattacharjee[1,2] and Anand K. Jha[1,*]

[1]Department of Physics, Indian Institute of Technology Kanpur, Kanpur, UP 208016, India
[2]e-mail: arko.hkd@gmail.com
*Corresponding author: akjha9@gmail.com

Received 21 April 2020; revised 4 June 2020; accepted 19 June 2020; posted 22 June 2020 (Doc. ID 395697); published 15 July 2020

Structured fields that are spatially completely coherent have been extensively studied in the context of long-distance optical communication, as the structure in the intensity profile of such fields is used for encoding information. This method of doing optical communication works very well in the absence of turbulence. However, in the presence of turbulence, the intensity structures of such fields start to degrade because of the complete spatial coherence of the field, and this structural degradation increases with the increase in turbulence strength. On the other hand, several theoretical studies have now shown that the structured fields that are spatially only partially coherent are less affected by turbulence. However, to the best of our knowledge, no such experimental demonstration has been reported until now. In this Letter, we experimentally demonstrate the structural robustness of partially coherent fields in the presence of turbulence, and we show that for a given turbulence strength, the structural robustness of a partially coherent field increases as the spatial coherence length of the field is decreased.

https://doi.org/10.1364/OL.395697

In the past few decades, structured fields that are spatially completely coherent, such as Laguerre Gaussian (LG) and Hermite Gaussian (HG) modes produced by stable laser resonators [1] or spatial light modulators (SLMs) [2], have gained importance due to their implications for optical communication [3–7]. The structure in the intensity profile of such fields is used for encoding information in the long-distance fiber [8] and free-space [9–11] optical communication. However, the problem of using such structured fields in the presence of a turbulent medium is that the medium introduces random phase fluctuations at different spatial locations in the field, and due to the perfect spatial coherence of the field, these random phase fluctuations result in degradation of the intensity structures of such fields. As a consequence, the retrieval of information encoded in the intensity structures becomes difficult. For this reason, the structures in a spatially perfectly coherent field become unsuitable for optical communication in turbulent environments.

On the other hand, it is now known that a spatially partially coherent field is less affected by turbulence [12–16]. Furthermore, theoretical studies have now shown that in the presence of turbulent environments, the structures in the intensity profiles and in the cross-spectral density functions of a spatially partially coherent field degrade less in comparison to the intensity structures of a spatially perfectly coherent field [17–21]. This implies that the structural robustness of the intensity profiles and the cross-spectral density functions of a spatially partially coherent field could be utilized towards optical communication even in the presence of a turbulent environment. Although in the past few years, there has been a growing interest in engineering various structured fields that are spatially partially coherent [22–26], to the best of our knowledge, no experimental demonstration of structural robustness of the cross-spectral density function of such fields in turbulence has been reported so far. In this Letter, we experimentally demonstrate structural robustness of partially coherent fields in turbulent environments. Simulating planar turbulence with the help of an SLM, we show that for a given turbulence strength, the structural robustness of a partially coherent field increases as the spatial coherence length of the field is decreased.

Figure 1 shows the schematic of our experimental setup and also illustrates how our structured partially coherent source propagates through a planar simulated turbulence and gets detected. In our experimental demonstrations, we use the scheme in Ref. [27] for generating spatially partially coherent fields with structures in their cross-spectral density functions. A planar, monochromatic, spatially completely incoherent primary source is kept at the back focal plane $z = -F$ of a lens located at $z = 0$. The central wavelength of the source is $\lambda_0 = 2\pi/k_0$, where k_0 is the magnitude of the wavevector. The combination of the primary incoherent source along with the lens constitutes our structured spatially partially coherent source. The structured partially coherent field passes through a planar simulated turbulence kept at $z = z'$ and then gets observed by the detection system consisting of a converging lens of focal length f kept at $z = z_d$ and a camera kept at $z = z_f = z_d + f$. The detection system essentially measures the cross-spectral density function of the field at $z = z_d$. We represent the transverse position coordinates at $z = -F$, $z = z'$,

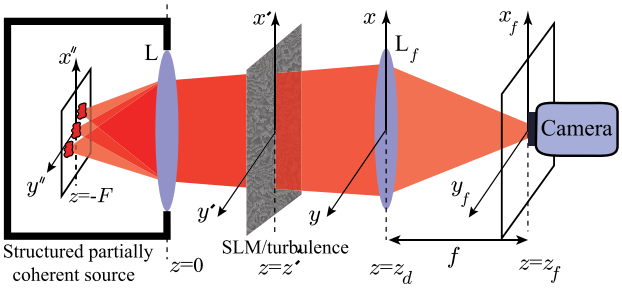

Fig. 1. Schematic of the experimental setup illustrating propagation of our structured partially coherent field through a turbulent medium.

$z=z_d$, and $z=z_f$ by $\boldsymbol{\rho}''\equiv(x'', y'')$, $\boldsymbol{\rho}'\equiv(x', y')$, $\boldsymbol{\rho}\equiv(x, y)$, and $\boldsymbol{\rho}_f\equiv(x_f, y_f)$, respectively. The intensity of the primary source at $z=-F$ is given by $I(\boldsymbol{\rho}'', z=-F)$. Therefore, the cross-spectral density function $W_s(\boldsymbol{\rho}_1', \boldsymbol{\rho}_2'; z=z')$ of our partially coherent field at $z=z'$ can be shown to be [27]

$$W_s(\boldsymbol{\rho}_1', \boldsymbol{\rho}_2'; z=z') \rightarrow W_s(\Delta\rho'; z=z') = \frac{A}{F^2}\iint I(\boldsymbol{\rho}''; z=-F)e^{-i\frac{k_0}{F}\boldsymbol{\rho}''\cdot\Delta\boldsymbol{\rho}'}\mathrm{d}\boldsymbol{\rho}'', \tag{1}$$

where $\Delta\rho'=|\boldsymbol{\rho}_2'-\boldsymbol{\rho}_1'|$. We note that the cross-spectral density function $W_s(\boldsymbol{\rho}_1', \boldsymbol{\rho}_2'; z=z')$ of our source depends on the transverse coordinates only through their difference $\Delta\rho'$. Therefore, we write it as $W_s(\Delta\rho'; z=z')$. Such sources are referred to as statistical homogeneous sources [28] or even spatially stationary sources [27]. The cross-spectral density $W(\boldsymbol{\rho}_1', \boldsymbol{\rho}_2'; z=z')$ at $z=z'$ right after the turbulence plane is given by $W(\boldsymbol{\rho}_1', \boldsymbol{\rho}_2'; z=z') = W_s(\Delta\rho'; z=z')W_t(\boldsymbol{\rho}_1', \boldsymbol{\rho}_2')$, where $W_t(\boldsymbol{\rho}_1', \boldsymbol{\rho}_2')$ is the cross-spectral density induced due to the turbulence. According to the Kolmogorov model,

$$W_t(\boldsymbol{\rho}_1', \boldsymbol{\rho}_2') = e^{-3.44\left(\frac{\Delta\rho'}{r_0}\right)^{\frac{5}{3}}}. \tag{2}$$

The quantity r_0 is called Fried's coherence diameter [29,30], and it quantifies the strength of turbulence. The value of r_0 ranges from 0 to ∞, with limit $r_0\rightarrow 0$ implying infinite turbulence strength and limit $r_0\rightarrow\infty$ implying no turbulence. In order to show the structural robustness of our partially coherent field in turbulence, we obtain the cross-spectral density function of the field after it has propagated up to $z=z_d$. Using Eqs. (1) and (2) and the Wolf propagation equation (section 4.4.3 in Ref. [28]), we find the cross-spectral density function $W(\boldsymbol{\rho}_1, \boldsymbol{\rho}_2; z=z_d)\rightarrow W(\Delta\rho; z=z_d)$ at $z=z_d$ to be

$$W(\Delta\rho; z=z_d) = e^{-3.44\left(\frac{\Delta\rho}{r_0}\right)^{\frac{5}{3}}} W_s(\Delta\rho; z=z_d), \tag{3}$$

where

$$W_s(\Delta\rho; z=z_d) = \frac{A}{F^2}\iint I(\boldsymbol{\rho}''; z=-F)e^{-i\frac{k_0}{F}\boldsymbol{\rho}''\cdot\Delta\rho}\mathrm{d}\boldsymbol{\rho}'' \tag{4}$$

is the cross-spectral density function of the field at $z=z_d$ in the absence of turbulence, and $\Delta\rho=|\boldsymbol{\rho}_2-\boldsymbol{\rho}_1|$. We note that the cross-spectral density functions $W(\Delta\rho; z=z_d)$ and $W_s(\Delta\rho; z=z_d)$ depend on the transverse position coordinates only through their difference $\Delta\rho$ and thus that the field at $z=z_d$ remains spatially stationary with or without turbulence. Furthermore, we note that $W_s(\Delta\rho; z=z_d)$ remains propagation invariant [27], and therefore it has the same functional form as that of the cross-spectral density function $W_s(\Delta\rho; z=z')$ given in Eq. (1). We note that since $W(\Delta\rho; z=z_d)$ is spatially stationary, it can be expressed in terms of the intensity $I(\rho_f; z=z_f)$ at $z=z_f$. In order to show this, we first write the cross-spectral density $W_l(\boldsymbol{\rho}_1, \boldsymbol{\rho}_2; z=z_d)$ at $z=z_d$ right after the lens L_f as $W_l(\boldsymbol{\rho}_1, \boldsymbol{\rho}_2; z=z_d) = W(\Delta\rho; z=z_d)\,T^*(\boldsymbol{\rho}_1)\,T(\boldsymbol{\rho}_2)$, where $T(\boldsymbol{\rho}) = e^{i\frac{k_0}{2f}\rho^2}$ is the transmission function of lens L_f [31]. Next, using the Wolf propagation equation [28], we propagate the field from $z=z_d$ to $z=z_f$ and find the intensity $I(\boldsymbol{\rho}_f; z=z_f)$ at $z=z_f$ plane to be

$$I(\boldsymbol{\rho}_f; z=z_f) = W(\boldsymbol{\rho}_f, \boldsymbol{\rho}_f; z=z_f) = \iint W(\Delta\rho; z=z_d)e^{i\frac{k_0}{f}\boldsymbol{\rho}_f\cdot\Delta\boldsymbol{\rho}}\mathrm{d}\Delta\boldsymbol{\rho}. \tag{5}$$

We Fourier-invert Eq. (5) and write it as

$$W(\Delta\rho; z=z_d) = \iint I(\boldsymbol{\rho}_f; z=z_f)e^{-i\frac{k_0}{f}\boldsymbol{\rho}_f\cdot\Delta\rho}\mathrm{d}\boldsymbol{\rho}_f. \tag{6}$$

Thus we see that by measuring the intensity $I(\rho_f; z=z_f)$ at the focal plane $z=z_f$, one obtains the cross-spectral density function $W(\Delta\rho, z=z_d)$ at $z=z_d$.

We next present our experimental demonstration of structural robustness of spatially partially coherent fields in the presence of turbulence. Figure 1 shows the schematic of the experimental setup, where the structured partially coherent source is kept at $z=0$. We use an SLM for simulating planar turbulence at $z=z'$ [32] and an electron multiplied charged coupled device (EMCCD) camera for measuring the intensity at $z=z_f$ plane. From Eq. (4), we have that the cross-spectral density function $W_s(\Delta\rho; z=z_d)$ at $z=z_d$ is the Fourier transform of the intensity $I(\boldsymbol{\rho}''; z=-F)$ of the primary incoherent source. Therefore, in order to generate a spatially partially coherent field with a structured cross-spectral density function, we use a light emitting diode (LED) array as our primary source. The array consists of nine LEDs arranged in a 3×3 grid. The size of the individual LED is $a=0.58$ mm. Figure 2(a) shows the simulated intensity $I(\boldsymbol{\rho}''; z=-F)$ of our primary incoherent source at $z=-F$, while Fig. 2(b) shows the corresponding cross-spectral density function $W_s(\Delta\rho; z=z_d)$ at $z=z_d$. We note that the oscillatory features of the cross-spectral density function in Fig. 2(b) decays over a length scale σ_c in the transverse direction. Using Eq. (4), it can be shown that σ_c is decided by the transverse size a of the individual LEDs at $z=-F$ and

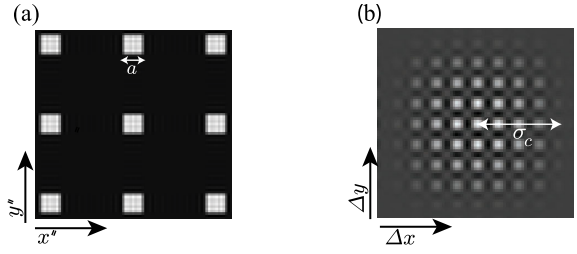

Fig. 2. (a) Simulated intensity of the primary source. (b) Simulated cross-spectral density $W_s(\Delta\rho; z=z_d)$ of the source at $z=z_d$.

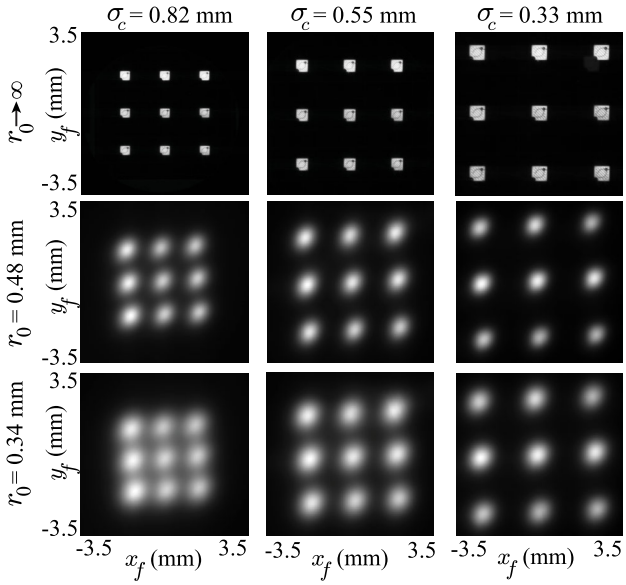

Fig. 3. Experimentally measured $I(\boldsymbol{\rho}_f; z = z_f)$ with different transverse coherence lengths at various turbulence strengths.

that it can be written as $\sigma_c = \lambda_0 F/a$ (see Ref. [28], section 4.4.4). We take σ_c as the spatial coherence length of the field. This definition of the spatial coherence length is consistent with the definition of temporal coherence length for a multimode continous-wave (CW) laser with a structured temporal cross-spectral density function [33]. By using lenses of focal lengths $F = 30$ cm, 50 cm, and 75 cm in the source configuration, we generate structured spatially partially coherent fields with $\sigma_c = 0.33$ mm, 0.55 mm, and 0.82 mm, respectively. In order to simulate turbulence using an SLM kept at $z = z'$, we display around 200 random phase patterns on the SLM with Kolmogorov statistics in a sequential manner at a frame rate of 30 Hz. We set an exposure time of 7 s such that the EMCCD camera records the entire ensemble of fields corresponding to the 200 phase patterns. We perform experiments at three different turbulence strengths $r_0 \to \infty$, $r_0 = 0.48$ mm, and $r_0 = 0.34$ mm.

In our experiments, we use $f = 30$ cm, $z' = 20$ cm, $z_d = 50$ cm, and $z_f = z_d + f = 80$ cm. Figure 3 shows the experimentally measured intensity $I(\boldsymbol{\rho}_f; z = z_f)$ at $z = z_f$ for different spatial coherence lengths σ_c at various turbulence strengths r_0. With no turbulence, that is, at $r_0 \to \infty$, the intensity $I(\boldsymbol{\rho}_f; z = z_f)$ at different σ_c is same as the intensity $I(\boldsymbol{\rho}''; z = -F)$ of the primary source shown in Fig. 2(a), apart

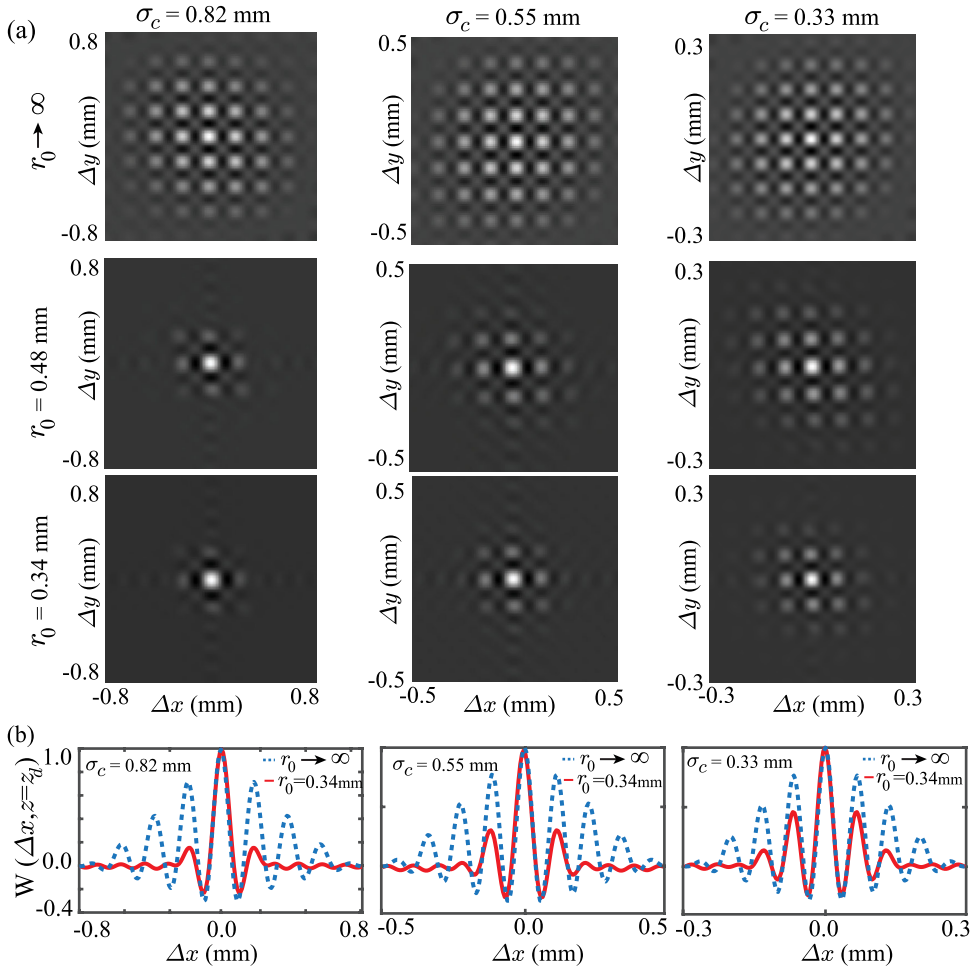

Fig. 4. (a) Reconstructed cross-spectral density function $W(\Delta\rho; z = z_d)$ for different transverse coherence lengths at various turbulence strengths. (b) Plots of one-dimensional cuts along the x direction of $W(\Delta\rho; z = z_d)$ at $r_0 \to \infty$ and $r_0 = 0.34$ mm for different σ_c.

from a change in scale. In the presence of turbulence, we find that as the spatial coherence length σ_c of the field decreases from 0.82 mm to 0.33 mm, the degradation in the structural features of the intensity $I(\boldsymbol{\rho}_f; z = z_f)$ becomes lesser. The small tilt in the measured intensity in Fig. 3 is attributed to the imperfections in the alignment of the experimental setup.

Next, using Eq. (6), we reconstruct the cross-spectral density function $W(\Delta\rho; z = z_d)$ at $z = z_d$ from the above measured intensity $I(\boldsymbol{\rho}_f; z = z_f)$. Figure 4(a) shows the reconstructed cross-spectral density function $W(\Delta\rho; z = z_d)$ at $z = z_d$ for different σ_c at various r_0. We see that in the absence of turbulence, that is, at $r_0 \to \infty$, the two-dimensional structure profile of $W(\Delta\rho; z = z_d)$ is same for all three σ_c values, apart from a change in scale. In the presence of turbulence, we find that the two-dimensional structures suffer degradation for all three σ_c values. However, at a given turbulence strength, the structural degradation becomes less as the spatial coherence length is decreased. We note that in Fig. 4(a), we have plotted $W(\Delta\rho; z = z_d)$ over different ranges of $\Delta\rho = (\Delta x, \Delta y)$ at different σ_c. This is so that we can better compare the structural degradation at different σ_c values. Finally, in order to highlight the main claim of this Letter, which is that the structural robustness increases as σ_c in decreased, we plot in Fig. 4(b) the one-dimensional cross-spectral density function $W(\Delta x; z = z_d)$ by taking one-dimensional cuts of $W(\Delta\rho; z = z_d)$ plots in Fig. 4(a). For each σ_c, we plot $W(\Delta x; z = z_d)$ at $r_0 \to \infty$, and $r_0 = 0.34$ together. These plots clearly show that the structural robustness of the cross-spectral density function of a spatially partially coherent field increases as we decrease the spatial coherence length of the field.

In conclusion, we have experimentally demonstrated structural robustness of spatially partially coherent fields in the presence of turbulence. We have shown that at a given turbulence strength, the structural robustness of a partially coherent field increases with the decrease in the spatial coherence length of the field. Our work can have important implications for long-distance optical communication through turbulent environments. We note that in our experiments, we have worked with simulated planar turbulence of strength r_0 ranging from ∞ to 0.34 mm. On the other hand, for real atmospheric turbulence, although the typical values of r_0 range from 4 mm to 30 mm [3,9,10], the turbulence is distributed and can even cause amplitude fluctuations. Nevertheless, we expect the main result of this Letter to remain qualitatively valid even for real atmospheric turbulence. We further note that the scheme presented in this Letter for measuring the cross-spectral density function works only for spatially stationary partially coherent fields. However, there are non-spatially stationary partially coherent fields with interesting propagation properties [34]. We expect even these fields to show structural robustness in turbulence.

Funding. Science and Engineering Research Board (EMR/2015/001931); Department of Science and Technology, Goverment of India (DST/ICPS/QuST/Theme- 1/2019).

Acknowledgment. We thank Shaurya Aarav for useful discussions.

Disclosures. The authors declare no conflicts of interest.

REFERENCES

1. A. Forbes, Laser Photon. Rev. **13**, 1900140 (2019).
2. N. Matsumoto, T. Ando, T. Inoue, Y. Ohtake, N. Fukuchi, and T. Hara, J. Opt. Soc. Am. A **25**, 1642 (2008).
3. M. P. Lavery, C. Peuntinger, K. Günthner, P. Banzer, D. Elser, R. W. Boyd, M. J. Padgett, C. Marquardt, and G. Leuchs, Sci. Adv. **3**, e1700552 (2017).
4. A. Trichili, A. B. Salem, A. Dudley, M. Zghal, and A. Forbes, Opt. Lett. **41**, 3086 (2016).
5. V. Aksenov, V. Kolosov, and C. Pogutsa, J. Opt. **15**, 044007 (2013).
6. M. A. Cox, L. Cheng, C. Rosales-Guzmán, and A. Forbes, Phys. Rev. Appl. **10**, 024020 (2018).
7. K. Pang, H. Song, Z. Zhao, R. Zhang, H. Song, G. Xie, L. Li, C. Liu, J. Du, A. F. Molisch, M. Tur, and A. E. Willner, Opt. Lett. **43**, 3889 (2018).
8. L. Zhu, J. Liu, Q. Mo, C. Du, and J. Wang, Opt. Express **24**, 16934 (2016).
9. M. Krenn, R. Fickler, M. Fink, J. Handsteiner, M. Malik, T. Scheidl, R. Ursin, and A. Zeilinger, New J. Phys. **16**, 113028 (2014).
10. M. Krenn, J. Handsteiner, M. Fink, R. Fickler, R. Ursin, M. Malik, and A. Zeilinger, Proc. Natl. Acad. Sci. USA **113**, 13648 (2016).
11. M. Erhard, R. Fickler, M. Krenn, and A. Zeilinger, Light Sci. Appl. **7**, 17146 (2018).
12. H. Roychowdhury and E. Wolf, Opt. Commun. **241**, 11 (2004).
13. S. Avramov-Zamurovic, C. Nelson, S. Guth, O. Korotkova, and R. Malek-Madani, Opt. Commun. **359**, 207 (2016).
14. J. C. Ricklin and F. M. Davidson, J. Opt. Soc. Am. A **19**, 1794 (2002).
15. M. Salem, T. Shirai, A. Dogariu, and E. Wolf, Opt. Commun. **216**, 261 (2003).
16. M. Wang, X. Yuan, and D. Ma, Appl. Opt. **56**, 2851 (2017).
17. Z. Mei, E. Shchepakina, and O. Korotkova, Opt. Express **21**, 17512 (2013).
18. J. Yu, F. Wang, L. Liu, Y. Cai, and G. Gbur, Opt. Express **26**, 16333 (2018).
19. J. Zhu, X. Li, H. Tang, and K. Zhu, Opt. Express **25**, 20071 (2017).
20. X. Liu, J. Yu, Y. Cai, and S. A. Ponomarenko, Opt. Lett. **41**, 4182 (2016).
21. R. Lin, H. Yu, X. Zhu, L. Liu, G. Gbur, Y. Cai, and J. Yu, Opt. Express **28**, 7152 (2020).
22. C. Liang, X. Zhu, C. Mi, X. Peng, F. Wang, Y. Cai, and S. A. Ponomarenko, Opt. Lett. **43**, 3188 (2018).
23. Y. Chen, S. A. Ponomarenko, and Y. Cai, Appl. Phys. Lett. **109**, 061107 (2016).
24. Y. Chen, F. Wang, C. Zhao, and Y. Cai, Opt. Express **22**, 5826 (2014).
25. Y. Cai, Y. Chen, and F. Wang, J. Opt. Soc. Am. A **31**, 2083 (2014).
26. C. Liang, F. Wang, X. Liu, Y. Cai, and O. Korotkova, Opt. Lett. **39**, 769 (2014).
27. S. Aarav, A. Bhattacharjee, H. Wanare, and A. K. Jha, Phys. Rev. A **96**, 033815 (2017).
28. L. Mandel and E. Wolf, *Optical Coherence and Quantum Optics* (Cambridge University 1995).
29. D. L. Fried, J. Opt. Soc. Am. **56**, 1372 (1966).
30. R. W. Boyd, B. Rodenburg, M. Mirhosseini, and S. M. Barnett, Opt. Express **19**, 18310 (2011).
31. J. W. Goodman, *Introduction to Fourier Optics* (Roberts and Company, 2005).
32. B. Rodenburg, M. P. Lavery, M. Malik, M. N. O'Sullivan, M. Mirhosseini, D. J. Robertson, M. Padgett, and R. W. Boyd, Opt. Lett. **37**, 3735 (2012).
33. L. Mandel and E. Wolf, Proc. Phys. Soc. London **80**, 894 (1962).
34. X. Li, S. A. Ponomarenko, Z. Xu, F. Wang, Y. Cai, and C. Liang, Opt. Lett. **45**, 698 (2020).